



Aerosol Optical Depth Retrievals over Thick Smoke Aerosols using GOES-17

Zhixin Xue¹ and Sundar A. Christopher¹

¹Department of Atmospheric and Earth Science, University of Alabama in Huntsville, USA

Correspondence: Zhixin Xue (zhixin.xue@uah.edu)

Abstract.

Severe wildfires generate thick smoke plumes, which degrade particulate matter air quality near the surface. Satellite measurements provide spectacular views of these smoke aerosols and Aerosol Optical Depth (AOD), a columnar measure of aerosol concentration widely used in assessing air quality near the surface. However, these thick smoke plumes often go undetected in satellite imagery, creating missing gaps in these high-pollution areas. In this study, we develop a new algorithm to detect and retrieve AOD from GOES-17 and compare these estimates with the Aerosol Robotic Network (AERONET), MODIS Multi-Angle Implementation of Atmospheric Correction (MAIAC), and the current GOES Operational Aerosol Optical Depth (OAOD) product. Using the clear-sky reflectance composite approach to retrieve surface reflectance, AOD accuracy increases 2% - 7% on different days for optically thin aerosols. We also found that adding information from the red channel in AOD retrieval brings more uncertainties for low AOD retrieval but increased accuracy for high AOD retrieval. After relaxing the maximum detectable AOD values, the number of valid AOD retrievals increases by 80%, and the accuracy also increases by about 4% compared to AERONET AOD. Our approach to retrieving AOD has a 386,091 ~ 937,210 square kilometer increase in valid AOD values each day.

1 Introduction

Geostationary satellite observations have the potential to improve exposure estimates since it has higher temporal resolution and 28% more data than Moderate Resolution Imaging Spectroradiometer (MODIS) observations for air quality applications (Paciorek et al., 2008). However, missing retrievals in Geostationary Operational Environmental Satellites (GOES) Operational Aerosol Optical Depth (OAOD) for thick smoke conditions are major limitations for tracking and studying smoke from fires (Huff et al., 2021). Missing retrievals of AOD during wildfire events are usually due to two reasons: cloud contamination and removal of high AOD values since the maximum valid AOD value is usually set to be 5 (Huff et al., 2021; Van Donkelaar et al., 2011). For the first condition, thick smoke tends to have larger spatial variances than thin aerosols and thus are often misclassified as clouds (Huff et al., 2021; Van Donkelaar et al., 2011). The second condition is also common for massive biomass burning events where the upper limits for AOD retrieval largely restrict the thick smoke retrieval (Eck et al., 2019). Therefore, during wildfire events, AOD retrievals are usually done by relaxing the thresholds for spatial variation and maximum AOD (Van Donkelaar et al., 2011).



The AErosol RObotic NETwork (AERONET) provides the ground-truth AOD measurements which are usually used to validate the satellite retrieved AOD values (Eck et al., 2019; Giles et al., 2019). When comparing with AERONET AOD, the NOAA Advanced Baseline Imager (ABI) AOD has similar bias and RMSE as the MODIS DT (dark target) AOD but lower correlation (Zhang et al., 2020; Gupta et al., 2018). However, the Multi-Angle Implementation of Atmospheric Correction (MAIAC) AOD improves the accuracy of the DT algorithm by about 15% (Lyapustin et al., 2018).

Previous studies have shown that GOES AOD biases mainly come from the limitations in the surface reflectance retrieval for relative thin aerosol loadings (Zhang et al., 2020). The current GOES operational algorithm (OAOD) first estimates the surface reflectance using the empirical relationships between 0.47 and 2.25 μm channels, and then performs the simultaneous retrievals of 550nm AOD and surface reflectance using 0.47, 0.64 and 2.25 μm channels (ABI AOD, 2018). The advantage of this algorithm is that it allows changing surface reflectance within a short time period (She et al., 2018), while another popular way to retrieve surface reflectance is to create a composite of reference surface albedo for each pixel by assuming it remains the same value over a certain time window (Knapp et al., 2005; Kim et al., 2008, 2014). Surface reflectance plays a significant role in retrieving AOD especially for optically thin aerosols, while this influence decreases as aerosol loading increases (Zhang et al., 2001).

While the primary goal of this study is to develop an algorithm to retrieve AOD during extreme optically thick aerosol conditions during wildfire events using GOES-17 level 1b radiance data, we also assess the role of surface reflectance on optically thin aerosol retrievals. Therefore, instead of using empirical relationships (e.g. between 0.47 and 2.25 μm channels) we provide a different approach by constructing clear-sky reflectance composites to characterize the surface to see if this improves or degrades the accuracy of the OAOA product. Our algorithm also relaxes the maximum AOD value and retrieves 470nm and 640nm AOD separately to calculate 550nm AOD. We then use MODIS MAIAC and AERONET AOD to validate the new AOD retrievals. We also compare the three AOD products (MAIAC, GOES-17 OAOA, and the new AOD retrievals) in thick smoke regions.

2 Data and Study Area

Thick smoke cases from September 2020 over the western US are selected to detect smoke aerosols and to retrieve AOD values. The new AOD is then compared with OAOA, MAIAC, and AERONET AOD values to assess the differences. Therefore, data sets that will be used in this study include GOES-17 level 1b radiance data, level 2 AOD data, AERONET AOD, and MAIAC AOD data products.

2.1 Study area

The Western United States experienced a series of wildfires and smoke pollution in September 2020. Wildfires in California, Colorado, Oregon, Arizona, and Washington burned nearly 10.2M acres. In terms of land burned, 2020 has 3 of the top 4 and 5 of the top 10 largest fires in California since records began in 1932 (Center, 2020). The thick smoke plumes generated from the fires are often misclassified as non-aerosol in the GOES AOD products which leads to large amounts of missing AODs,



thereby making the quantitative estimation of pollution difficult (Zhang et al., 2020). Therefore, to assess this issue we select the study area over the western US (30-50° N, 100-130° W) during September 2020 where there were numerous active fires.

60 The cases that we selected for this study are from September 11th to 19th, 2020 at 20UTC.

The goal of this study is not to provide information on the diurnal nature of smoke or a CONUS-wide assessment of the problem. We simply provide a case-study-based approach to test the algorithm and compare it with various data sets.

2.1.1 GOES radiance and AOD data

Since the study area is the western US, we use radiance and AOD data from GOES-west (GOES-17) satellite and F3 (CONUS) mode (Greenwald et al., 2016). The temporal resolution is 5 minutes and the spatial resolution is 2 km. Several bands have spatial resolution of 0.5 to 2 km for radiance data, and we therefore re-sampled them to 2km resolution for convenience (so we can use the same resolution as the thermal-IR band to identify cloudy pixels). To keep the data analysis manageable, only a certain time (20UTC) is used for retrieving AOD for each day, and 45 days of GOES radiance data are used to derive a clear-sky surface reflectance map and provide information on surface albedo retrievals which is important for the AOD retrievals.

70 The reason for choosing 20UTC is due to the maximum solar forcing. The results are then compared with OAOD within low aerosol loading areas to check the performances of the two methods (clear-sky reflectance composite approach and joint retrieval of surface reflectance and 550nm AOD). The reflectance data is also used for retrieving AOD by searching for the closest reflectance values in the AOD look-up table derived from a Discrete Ordinate Radiative (SBDART) radiative transfer model (Ricchiazzi et al., 1998).

75 The Level 2 OAOD data of the same time (20UTC) of each day with 2 km resolution is compared with different surface observations and other satellite products to examine the percentage of AOD missing for thick smoke cases. Due to the limited surface observation, at certain locations, we used the OAOD product with a 30-min temporal resolution to calculate the total missing percentage during daytime. For those missing pixels, we checked the quality flag of the OAOD product to assess the reasons for no retrievals.

80 2.2 AERONET AOD

Version 3 AERONET level 2 AOD products during the study period are used to compare with GOES OAOD product to calculate the AOD missing percentage (Giles et al., 2019). The level 2 data uncertainties for overhead sun range from 0.01 in the visible and near-infrared to 0.02 in the ultraviolet, indicating that the spectral AOD obtained by direct sun observations in AERONET is extremely accurate (Eck et al., 1999). We select 15 AERONET stations within our study area that have observations during the wildfire event for this comparison. The AERONET stations are very limited in Northwestern US with only one station in Washington state while most of the stations are distributed in California (Arizona, Nevada, and Washington have 1 station each and California has 12). AERONET provides various information including the total optical depth of different wavelengths, AOD, and other components such as ozone, NO₂, and Rayleigh optical depths with a temporal resolution of approximately 5 minutes. We used 500nm AOD for the comparison which is the closest to 550nm AOD, and convert it to 550nm AOD using the empirical angstrom exponent for smoke aerosols. The maximum value for AERONET AOD measurements depends on the

90



optical air mass ($\sim \frac{1}{\cos(\text{zenithangle})}$) and thus are different at different locations. The max AOD can be calculated by $\text{AOD} \times m < 7$ where m is the optical air mass (Eck et al., 2019). For example, one AERONET station used in this study is PNNL (46.341° N, 119.279° W) which has a measurable AOD of around 5. While other stations with lower solar zenith angles have a max measurable AOD of about 6. Also, for some AERONET stations with high aerosol loading, AOD values are retained for longer wavelengths while no valid 500nm AOD is available for comparison in this study.

2.3 MAIAC AOD

MAIAC AOD (MCD19A2) that combines Aqua and Terra-MODIS AOD is used to validate the retrieved-AOD in this study (Lyapustin et al., 2018, 2011). The MAIAC AOD retrieval algorithm separates the contribution of aerosol and land reflection using time series data, and retrieves spectral regression coefficient (SRC) by finding the minimum ratio between blue and SWIR band, which can be used for calculating surface bidirectional reflectance distribution function (Lyapustin et al., 2018; Qin et al., 2021). The algorithm also detects smoke aerosols by calculating absorption parameter using deep blue and blue bands (412nm and 466nm). Then AOD is retrieved by minimization of a function that computes the ratio between measured and theoretical reflectance (Lyapustin et al., 2018). Note that the MAIAC AOD is derived using observations of MODIS Terra and MODIS Aqua at 1030 and 1400 local time respectively, while the GOES product used in this study is 1200 local time, so there might be some slight differences in the AOD distribution. The final AOD calculated from our approach (from now on RTM) will also be compared with MAIAC AOD.

3 Methods

In order to compare different surface albedo retrieval methods, we use the same internal tests in the GOES OAOD algorithm to mask out cloudy or snow pixels (ABI AOD, 2018). Instead of retrieving 550nm AOD and surface albedo at the same time, we calculate the clear-sky TOA (cloud and aerosol-free) reflectance calculated from 45-day of observations. Then we convert the TOA clear sky reflectance to surface values using the SBDART model (Zhang et al., 2001). Next, we construct the AOD look-up table according to different viewing, solar zenith, relative azimuth angles and improved surface albedo estimates. Finally, the new AOD is compared with MAIAC AOD and AERONET AOD.

To improve the AOD retrieval in thick smoke regions, we first check the quality flags of OAOD products to determine the main reasons for missing values at high aerosol loading regions. Then we relax the max value for AOD retrieval to allow higher values. The retrieval of 470nm and 640nm AOD are performed separately, and then we calculate the 550nm AOD by applying a log scale interpolation using 470nm and 640nm AOD.

3.1 Missing data in GOES AOD

For wildfire studies, AOD is an important variable for estimating surface pollution (Wang and Christopher, 2003), but the Geo-stationary satellite AOD values are often missing for optically thick smoke areas. Therefore, we first calculate the percentage of missing AOD due to the retrieval methods of GOES from September 11th to September 19th, 2020.



Due to the limited number of observations in the Northwest US, we first use all the AOD retrievals in the 9-day period of one sun photometer site in Washington state (PNNL-46.341°N, 119.279°W) to examine the missing percentage of GOES OAOD product. We test the missing percentage of AERONET stations using only one site (PNNL) for several reasons: first, the number of AERONET stations in the Northwestern US is limited; second, other stations have significant missing data gaps during this period. In order to estimate the missing percentage of GOES OAOD retrieval methods and to compare the satellite and ground observations, we average both the AERONET and GOES AOD every 3 hours. For GOES AOD, we average the AOD values every 3 hours with a time interval of 30 minutes (average 0000,0030,0100,0130...UTC) and average all points within 0.3-degree distances from the AERONET station. Note that we only average valid AOD values within the distances (missing AOD due to clouds will be discarded – AOD with fill values or QF is 3). Comparing the 500nm AERONET AOD with GOES AOD, we can easily assess the number of missing AOD from GOES. This spatiotemporal averaging of satellite with ground-based observations is consistent with previous approaches (Gupta et al., 2018).

To be consistent with our AOD derivation, we also calculate the GOES AOD missing percentage at 20UTC. The first step is to find the nearest GOES pixel for each station and take a 5×5 box around the pixel to calculate the mean AOD of all valid values. Then we compare the number of valid ground observations of the 15 stations during the 9-day period with the mean GOES AOD to calculate the missing percentage of OAOD.

3.2 Clear-sky surface reflectance

We use 45 days of radiance data (blue, red and 11 μm channel) to derive a TOA clear-sky reflectance map. For each pixel, we select the days that have the three lowest values at both red and blue channels, and choose the day with the highest brightness temperature at 11 μm channel if there is more than one day selected. We assume this clear-sky reflectance map is the TOA reflectance that includes the Rayleigh scattering from the atmosphere with nearly zero aerosol concentrations. Then we can obtain the surface albedo using the SBDART model by applying the mid-latitude summer atmospheric profile and generating a look-up table for surface albedo (Gupta et al., 2018). We use solar zenith angle and viewing zenith angle from 0 to 60 with an interval of 5 degrees, relative azimuth angle from 0 to 180 with an interval of 10 degrees, and surface albedo from 0 to 0.5 with an interval of 0.01 to calculate the TOA reflectance from the SBDART model. After obtaining the surface albedo from the look-up table, we can retrieve the corresponding surface albedo from the clear-sky reflectance map.

3.3 AOD retrieval

The processing outline of the AOD retrieval algorithm is summarized in Figure 1. We first mask out the cloudy, snow, and water pixels following the GOES algorithm (internal tests) by: a) setting a threshold at blue channel; b) performing spatial inhomogeneity test (3×3 standard deviations); c) calculating NDSI (normalized difference snow index) and set a threshold of 0.3; d) calculating the NDVI (normalized difference vegetation index) and set a threshold of 0.1 with another threshold at 0.86 μm channel of 0.1. Next, we generate the AOD look-up table using the SBDART model for different surface albedo and angles at blue and red channels, and we extend the max AOD value from 5 to 10. Then for non-cloudy pixels, we perform AOD retrievals using RTM to obtain the AOD values at blue and red channels. For each pixel, we use the corresponding solar zenith



155 angle, viewing zenith angle, relative azimuth angle and surface albedo calculated from the previous step. Finally, we calculate the 550nm AOD using 640nm and 470nm AOD by applying log scale interpolation (Lee and Chung, 2013):

$$AOD_{550} = AOD_{640}^{\frac{550-470}{(550-470)+(640-550)}} \times AOD_{470}^{1-\frac{640-550}{(550-470)+(640-550)}} \quad (1)$$

Before we use this log scale interpolation to calculate the 550nm AOD, we first tested it using AERONET 440nm, 500nm and 675nm AOD, and related statistics including correlation coefficients and median bias are calculated (statistics are shown in section 4.2). A simpler way to derive 550nm AOD is to use 470nm AOD directly with empirical Angstrom exponent for smoke (~ 2 , (Bian et al., 2020)):

$$AOD_{550} = AOD_{470} \times \left(\frac{550}{470}\right)^{-\alpha} \quad (2)$$

where α is the Angstrom exponent for smoke aerosol. The value of Angstrom exponent varies for different aerosol types and in different regions, and the decadal value for Pacific West is around 2.24 while around 1.91 in the Southeastern US (Bian et al., 2020). Therefore, here we choose 2 to represent the smoke aerosols in the western US. Both methods are validated with MAIAC AOD and AERONET AOD.

4 Results

We first discuss the percentage of missing values of satellite observations due to the retrieval methods. Then we retrieve the surface albedo by calculating a clear-sky TOA reflectance of the study region using reflectance values of 45-days data. According to the newly retrieved surface reflectance, we can retrieve AOD at red and blue channels. Since surface reflectance has a larger effect on AOD at low aerosol loading regions, we compare the two surface reflectance retrieval methods (the clear-sky reflectance composite approach and OAOD algorithm) by validating lower AOD values ($AOD < 1$) with MAIAC and AERONET AOD. For high aerosol loading regions, we combine the red and blue channel AOD to calculate the 550nm AOD and validate it with AERONET AOD.

4.1 Descriptive statistics of ground measurements and satellite data

Figure 2 shows the RGB image of a wildfire event in the western US from September 11th to 19th 2020 at 20UTC. The fire sources are located in California and Oregon, and the smoke is transported further north to Washington. Since GOES-R does not have the green band, we use $0.45 \times \text{red} + 0.1 \times \text{veggie} + 0.45 \times \text{blue}$ to calculate a "fake" green channel to show the RGB image (red- $0.67\mu\text{m}$ channel, veggie- $0.86\mu\text{m}$ channel, blue- $0.47\mu\text{m}$ channel) (Bah et al., 2018). Note that these images are at 2km spatial resolution and are just for visualization purposes since we use a common spatial resolution of 2km for all our analysis.

Figure 3 shows the corresponding AOD values from the GOES level 2 product, and it is clear that in comparison with figure 2, there are large areas of missing AOD values in the thick smoke region where the pollution should be highest, especially on



September 11th, 12th, and 17th. The black circles indicate the areas of missing AOD. Therefore, as the first step of this study, we roughly assess the missing percentage of OAOD by comparing it with AERONET AOD observations in the smoke region.

185 Figure 4 shows the 3-hour average and 0.3-degree spatial average 550nm AOD comparisons between the PNNL AERONET station and OAOD for 9 days. Since the two AOD retrievals are not at the same wavelengths, we use the Angstrom exponent of 2 to indicate the reference line (Alados-Arboledas et al., 2011). The OAOD and ground AOD match well, however, the satellite measurements have a larger standard deviation which may be caused by the spatial variations of aerosols. Compared to AERONET, the GOES OAOD tends to overestimate when AOD is less than 3 while underestimating when AOD is larger than
 190 3. The total number of OAOD values is 40 while the surface only has 31 observations, and the main reason for this difference is that AERONET usually starts measuring AOD later than GOES-reported values. If we check the hourly measurement rather than the 3-hour average and without spatial averaging, GOES has 34 observations while AERONET has 49. This indicates the missing percentage of GOES measurements is approximately 31%. We also calculated the missing percentage of GOES AOD only for 20UTC using 15 different AERONET stations, and there are 111 valid AERONET AOD while only 57 of the
 195 measurements have corresponding valid OAOD. Therefore, the missing percentage of optically thick smoke pixels is about 49% at 20UTC during wildfire events.

4.2 AOD retrieval

In order to retrieve AOD, we use similar aerosol properties as the GOES OAOD algorithm (shown in table 2). The aerosol properties including particle radius, standard deviation of the radius, imaginary and real part of refractive index are used
 200 as inputs for MIE code to calculate other properties such as single scattering albedo, phase function, asymmetry factor and extinction efficiency. Then we use the SBDART model to generate a look-up table for AOD for different solar/viewing zenith angles and surface reflectance.

After retrieving 640nm and 470nm AOD, we used the log scale interpolation to obtain 550nm AOD. The method of using multi-wavelength AOD to calculate the AOD of a specific wavelength has been used in previous study (Lee and Chung, 2013).
 205 Therefore we performed a simple validation of the method using the 440nm, 500nm and 675nm AERONET AOD, and our calculated 500nm AOD matches well with measured values with correlation coefficient of 0.999 and median bias of 0.07.

4.3 550nm AOD calculated from 470nm AOD

As mentioned in the method section, there are two ways to calculate 550nm AOD: one is to calculate directly from 470nm AOD using the Angstrom exponent (hereafter AOD-angs) while another method is to combine 470nm and 640nm AOD (AOD-log).
 210 We found that AOD from the first method has a high correlation with MAIAC AOD and performs better in low aerosol loading regions. Figure 5 shows the AOD comparison of the regions with smoke aerosols between MAIAC, OAOD product and our new AOD-angs values. AOD-angs matches better with MAIAC AOD values while OAOD tends to be much higher. For both days, GOES OAOD data shows more variations according to the box and whisker plots. The large variances are most noticeable in the range of MAIAC AOD between 0.5 and 2, which may caused by the biases from surface albedo estimation. However,
 215 the horizontal linear features in the data points show that at different angles, the blue channel TOA reflectance becomes stable



(or insensitive) as AOD increases. We only show the AOD values whose corresponding values at 470nm AOD is less than 4 as we found that TOA reflectance becomes insensitive to AOD increasing over 4 under most circumstances. The statistics of the AOD comparisons are shown in table 3. Note that we selected the two days (September 13th and 17th) due to the large AOD missing areas in GOES OAOD product around Washington state, and we figured that the missing data is due to the large overestimation of OAOD product because our AOD retrievals indicate smaller values in this region (figure 5). However, in other days when smoke concentrated in different regions, AOD-angs also has larger AOD retrievals ($AOD > 4$).

There are a total of 15 AERONET stations within the study region that are used for validation, and MAIAC has the highest correlation ($R=0.9$) with AERONET while OAOD has the lowest correlation ($R=0.6$) (figure 6). Since AERONET AOD is only available at certain wavelengths, 500nm AOD is converted to 550nm AOD using Angstrom exponents of individual sites (calculated from 500nm and 675nm AOD). Statistics including root mean square error (RMSE), median bias, and accuracy within expected error ($EE: \pm(0.2+0.15AOD)$) are shown in table 4. We noticed that GOES OAOD product can retrieve high AOD values ($AOD > 2$) with relatively high accuracy while tending to have more noisy points in the lower AOD range. MAIAC AOD, on the other hand, has the highest accuracy in low aerosol loading regions where AOD is less than 1 while underestimating AOD in the high AOD range. AOD-angs shows higher accuracy when retrieving low AOD whereas large variations at a larger AOD range.

MAIAC AOD has high accuracy of around 66% within the expected error (EE) of $\pm 0.1AOD$ over the globe, but all the AOD values used for validation are lower than 2 (Lyapustin et al., 2018). Surface types also affect the accuracy of MAIAC AOD retrieval, and it was found that the accuracy is highest over forests but lowest over barren areas (Qin et al., 2021). Increased negative biases are found under high aerosol loading conditions, and the uncertainties of the MAIAC algorithm increase with aerosol loading (Qin et al., 2021; Martins et al., 2017). Also a recent study shows that the GOES OAOD product is found to have a diurnal bias caused by surface reflectance relationships, and the bias tends to be positive most of the time compared to AERONET AOD (Zhang et al., 2020).

One of the main difference between the three products is the wavelengths they use to retrieve 550nm AOD: MAIAC and AOD-angs uses 470nm reflectance to retrieve AOD; OAOD uses 470nm reflectance to retrieve 550nm AOD but then convert it to 640nm AOD using aerosol extinction coefficients to calculate the TOA reflectance at 640nm, and select the one with minimum residue at 640nm channel. Both methods using one short-wavelength have relatively high accuracy at low aerosol loading regions but fail to retrieve higher AOD values, which may be because reflectance at short-wavelengths becomes insensitive as AOD increases when AOD exceeds certain values. To check if it can improve the accuracy for retrieving high AOD values by making use of the red channel, we combine the AOD-angs with 640nm AOD to generate AOD-log to see if it performs better at high-value ranges.

4.4 550nm AOD calculated from 470nm and 640nm AOD

Combining both red and blue channel AOD, AOD-log shows larger variations (figure 7). The vertical linear features in figure 7 represent these values: 640nm AOD changes while 470nm AOD remains the same value. Therefore, adding information from the red channel increases the variations in low aerosol loading regions and slightly decreases the value of retrieved AOD.



250 Compared with AERONET AOD (shown in figure 6), variations are largest at AOD range from 1 to 2, but AOD-log can retrieve high AOD (>4) values with acceptable accuracy.

Figure 8 shows the new AOD at 550nm from September 11-19, 2020. Since we need to compare the results with MAIAC AOD which is 550nm AOD, we use log scale interpolation to combine both 470nm and 640nm AOD to calculate the 550nm AOD. Compared with the MAIAC AOD of the 9 days (figure 9), the distribution matches well except for some cloudy areas
 255 which are because MAIAC AOD combines both 1030 and 1400 local time AOD observations. Our results show that there are an increased number of AOD retrievals over thick smoke areas, and our new AOD has a 386,091 \sim 937,210 square kilometer increase on valid AOD values each day. Since we did not change the cloud screening process in the GOES OAOD algorithm, simply extending the max AOD value to 10 can increase a large portion of the missing values in OAOD. One thing to be noted is that MAIAC AOD has a max AOD of around 3.8 in the 9-day period though the spatial distribution is similar to our new
 260 AOD.

4.5 Uncertainties

There are several sources of uncertainties related to our study including the sensor biases, assumptions made for retrieving AOD and validation biases. The main uncertainties arise from:

1)When we compare the MAIAC AOD with the OAOD product, the distribution of smoke aerosol and clouds could be
 265 slightly different since the time of the two observations is different.

2)The 550 nm AOD is calculated by assuming the angstrom exponent for smoke aerosol is approximately 2, but it changes with different aerosol properties and with the smoke aging process.

3)The comparison between different satellite AOD and AERONET may be biased since the AERONET stations are not evenly distributed. Most of the AERONET stations are distributed in California while only one station is located in Washington
 270 state, thus constraining the surface types related to the VIS-SWIR relationships. Also, the measurable AOD for AERONET stations in higher latitudes is relatively low due to the high zenith angle, which may limited the validation at high AOD loading regions (the potential max AOD of 6.3 at the CA site versus a potential AOD max of 5.3 at the PNNL site).

4)For AOD validation, MAIAC AOD has a much higher correlation with AERONET AOD, and part of the reason is that the spatial resolution of MAIAC(1km) is finer than GOES (2km). We used a 5×5 -pixel box and take the mean AOD value from
 275 the satellite AOD to compare with AERONET AOD, therefore, MAIAC AOD has a smaller box size than GOES which could lead to a higher correlation.

5)All the three satellite AOD products used different radiative transfer models for retrieving AOD which may also bring uncertainties to the study. MAIAC uses SHARM, GOES uses 6S and we use the SBDART model.

6)45 days may be too long for generating the clear-sky reflectance composite in summer since the growth of plants can
 280 change the surface reflectance at shorter periods.



5 Conclusions

In this study, we assess the missing AOD percentage of the current version of GOES AOD during wildfire events using ground and satellite observations. Then we improve the surface reflectance retrieval methods and retrieve AOD for the thick smoke area. Finally, we compare our results with the MAIAC AOD observations. The main conclusion of our study:

- 285 1) By comparing the AERONET and GOES AOD from September 11th to 19th, 2020 at 20UTC, OAOD has approximately 49% missing values.
- 2) Our method provides 386,091 ~ 937,210 square km more detection and retrievals compared to GOES operational product.
- 3) The main reason for the OAOD product showing more variations when $AOD < 3$ is the use of a red channel which is necessary for retrieving surface reflectance and AOD at the same time. Retrieving the surface reflectance from the clear-sky
290 reflectance composite approach and retrieving AOD from the blue channel improves the AOD accuracy.
- 4) Our new AOD has increased the accuracy for OAOD and also increase the number of valid AOD observations by 80%. Our AOD has a higher correlation with both MAIAC and AERONET AOD.
- 5) To retrieve thick smoke aerosols, information from the red channel adds more accuracy than using only blue channel information.
- 295 Finally, we note that this is a case study-based approach from 45 days of GOES data at 20UTC to highlight a problem and develop solutions for detecting thick aerosols and retrieving AOD for these pixels. Future studies will provide a more comprehensive assessment of the diurnal nature of these issues over a much larger spatial scale that could be useful for climate and air quality studies.

Data availability. MAIAC AOD from Earthdata are available from <https://lpdaac.usgs.gov/products/mcd19a2v006/> (last access: 11 July
300 2022). GOES AOD from NOAA are available from <https://www.avl.class.noaa.gov/saa/products/catSearch> (last access: 11 July 2022). AERONET AOD are available from <https://aeronet.gsfc.nasa.gov/> (last access: 11 July 2022).

Code and data availability. SBDART model is available at <https://github.com/paulricchiazzi/SBDART> (last access: 11 July 2022).



References

- ABI AOD, A.: GOES-R Advanced Baseline Imager (ABI) algorithm theoretical basis document for suspended matter/aerosol optical depth
 305 and aerosol size parameter, Tech. rep., NOAA/NESDIS/STAR, Version 4.2, 14 February 2018, 2018.
- Alados-Arboledas, L., Müller, D., Guerrero-Rascado, J., Navas-Guzmán, F., Pérez-Ramírez, D., and Olmo, F.: Optical and microphysical
 properties of fresh biomass burning aerosol retrieved by Raman lidar, and star-and sun-photometry, *Geophysical Research Letters*, 38,
 2011.
- Bah, M., Gunshor, M., and Schmit, T.: Generation of GOES-16 True Color Imagery without a Green Band, *Earth and Space Science*, 5,
 310 549–558, 2018.
- Bian, Q., Ford, B., Pierce, J. R., and Kreidenweis, S. M.: A decadal climatology of chemical, physical, and optical properties of ambient
 smoke in the Western and Southeastern United States, *Journal of Geophysical Research: Atmospheres*, 125, e2019JD031 372, 2020.
- Center, G. A. C.: National large incident year-to-date report, National Interagency Fire Center, US, pp. 1–66, 2020.
- Eck, T., Holben, B., Giles, D., Slutsker, I., Sinyuk, A., Schafer, J., Smirnov, A., Sorokin, M., Reid, J., Sayer, A., et al.: AERONET remotely
 315 sensed measurements and retrievals of biomass burning aerosol optical properties during the 2015 Indonesian burning season, *Journal of*
Geophysical Research: Atmospheres, 124, 4722–4740, 2019.
- Eck, T. F., Holben, B., Reid, J., Dubovik, O., Smirnov, A., O’neill, N., Slutsker, I., and Kinne, S.: Wavelength dependence of the optical
 depth of biomass burning, urban, and desert dust aerosols, *Journal of Geophysical Research: Atmospheres*, 104, 31 333–31 349, 1999.
- Giles, D. M., Sinyuk, A., Sorokin, M. G., Schafer, J. S., Smirnov, A., Slutsker, I., Eck, T. F., Holben, B. N., Lewis, J. R., Campbell, J. R., et al.:
 320 Advancements in the Aerosol Robotic Network (AERONET) Version 3 database—automated near-real-time quality control algorithm with
 improved cloud screening for Sun photometer aerosol optical depth (AOD) measurements, *Atmospheric Measurement Techniques*, 12,
 169–209, 2019.
- Greenwald, T. J., Pierce, R. B., Schaack, T., Otkin, J., Rogal, M., Bah, K., Lenzen, A., Nelson, J., Li, J., and Huang, H.-L.: Real-time
 simulation of the GOES-R ABI for user readiness and product evaluation, *Bulletin of the American Meteorological Society*, 97, 245–261,
 325 2016.
- Gupta, P., Remer, L. A., Levy, R. C., and Mattoo, S.: Validation of MODIS 3 km land aerosol optical depth from NASA’s EOS Terra and
 Aqua missions, *Atmospheric Measurement Techniques*, 11, 3145–3159, 2018.
- Huff, A., Kondragunta, S., Zhang, H., Laszlo, I., Zhou, M., Caicedo, V., Delgado, R., and Levy, R.: Tracking Smoke from a Prescribed Fire
 and Its Impacts on Local Air Quality Using Temporally Resolved GOES-16 ABI Aerosol Optical Depth (AOD), *Journal of Atmospheric*
 330 *and Oceanic Technology*, 38, 963–976, 2021.
- Kim, J., Yoon, J.-M., Ahn, M., Sohn, B., and Lim, H.: Retrieving aerosol optical depth using visible and mid-IR channels from geostationary
 satellite MTSAT-1R, *International Journal of Remote Sensing*, 29, 6181–6192, 2008.
- Kim, M., Kim, J., Wong, M. S., Yoon, J., Lee, J., Wu, D., Chan, P., Nichol, J. E., Chung, C.-Y., and Ou, M.-L.: Improvement of aerosol
 optical depth retrieval over Hong Kong from a geostationary meteorological satellite using critical reflectance with background optical
 335 depth correction, *Remote sensing of environment*, 142, 176–187, 2014.
- Knapp, K. R., Frouin, R., Kondragunta, S., and Prados, A.: Toward aerosol optical depth retrievals over land from GOES visible radiances:
 determining surface reflectance, *International Journal of Remote Sensing*, 26, 4097–4116, 2005.
- Lee, K. and Chung, C. E.: Observationally-constrained estimates of global fine-mode AOD, *Atmospheric Chemistry and Physics*, 13, 2907–
 2921, 2013.



- 340 Lyapustin, A., Martonchik, J., Wang, Y., Laszlo, I., and Korkin, S.: Multiangle implementation of atmospheric correction (MAIAC): 1. Radiative transfer basis and look-up tables, *Journal of Geophysical Research: Atmospheres*, 116, 2011.
- Lyapustin, A., Wang, Y., Korkin, S., and Huang, D.: MODIS collection 6 MAIAC algorithm, *Atmospheric Measurement Techniques*, 11, 5741–5765, 2018.
- Martins, V. S., Lyapustin, A., de Carvalho, L. A., Barbosa, C. C. F., and Novo, E. M. L. d. M.: Validation of high-resolution MAIAC aerosol product over South America, *Journal of Geophysical Research: Atmospheres*, 122, 7537–7559, 2017.
- 345 Paciorek, C. J., Liu, Y., Moreno-Macias, H., and Kondragunta, S.: Spatiotemporal associations between GOES aerosol optical depth retrievals and ground-level PM_{2.5}, *Environmental science & technology*, 42, 5800–5806, 2008.
- Qin, W., Fang, H., Wang, L., Wei, J., Zhang, M., Su, X., Bilal, M., and Liang, X.: MODIS high-resolution MAIAC aerosol product: Global validation and analysis, *Atmospheric Environment*, 264, 118 684, 2021.
- 350 Ricchiuzzi, P., Yang, S., Gautier, C., and Sowle, D.: SBDART: A research and teaching software tool for plane-parallel radiative transfer in the Earth’s atmosphere, *Bulletin of the American Meteorological Society*, 79, 2101–2114, 1998.
- She, L., Xue, Y., Yang, X., Leys, J., Guang, J., Che, Y., Fan, C., Xie, Y., and Li, Y.: Joint retrieval of aerosol optical depth and surface reflectance over land using geostationary satellite data, *IEEE Transactions on Geoscience and Remote Sensing*, 57, 1489–1501, 2018.
- Van Donkelaar, A., Martin, R. V., Levy, R. C., da Silva, A. M., Krzyzanowski, M., Chubarova, N. E., Semutnikova, E., and Cohen, A. J.: 355 Satellite-based estimates of ground-level fine particulate matter during extreme events: A case study of the Moscow fires in 2010, *Atmospheric Environment*, 45, 6225–6232, 2011.
- Wang, J. and Christopher, S. A.: Intercomparison between satellite-derived aerosol optical thickness and PM_{2.5} mass: Implications for air quality studies, *Geophysical research letters*, 30, 2003.
- Zhang, H., Kondragunta, S., Laszlo, I., and Zhou, M.: Improving GOES Advanced Baseline Imager (ABI) aerosol optical depth (AOD) 360 retrievals using an empirical bias correction algorithm, *Atmospheric Measurement Techniques*, 13, 5955–5975, 2020.
- Zhang, J., Christopher, S. A., and Holben, B. N.: Intercomparison of smoke aerosol optical thickness derived from GOES 8 imager and ground-based Sun photometers, *Journal of Geophysical Research: Atmospheres*, 106, 7387–7397, 2001.

FIGURES

TABLES

AERONET (latlon)	PM2.5(latlon)	FRM/FEM?	Distance (km)
46.34° N, 119.28° W	46.58° N, 119° W	No	33.65
46.34° N, 119.28° W	46.2° N, 119.2° W	No	14.82

Table 1. location of AERONET and EPA PM_{2.5} stations (one AERONET station and two EPA stations)

$R_v(\mu m)$	$\sigma_v(\mu m)$	n_i	n_r
0.1335+0.0096 τ	0.3834+0.0794 τ	1.47	0.02

Table 2. Aerosol properties used for retrieving AOD (inputs for MIE code)

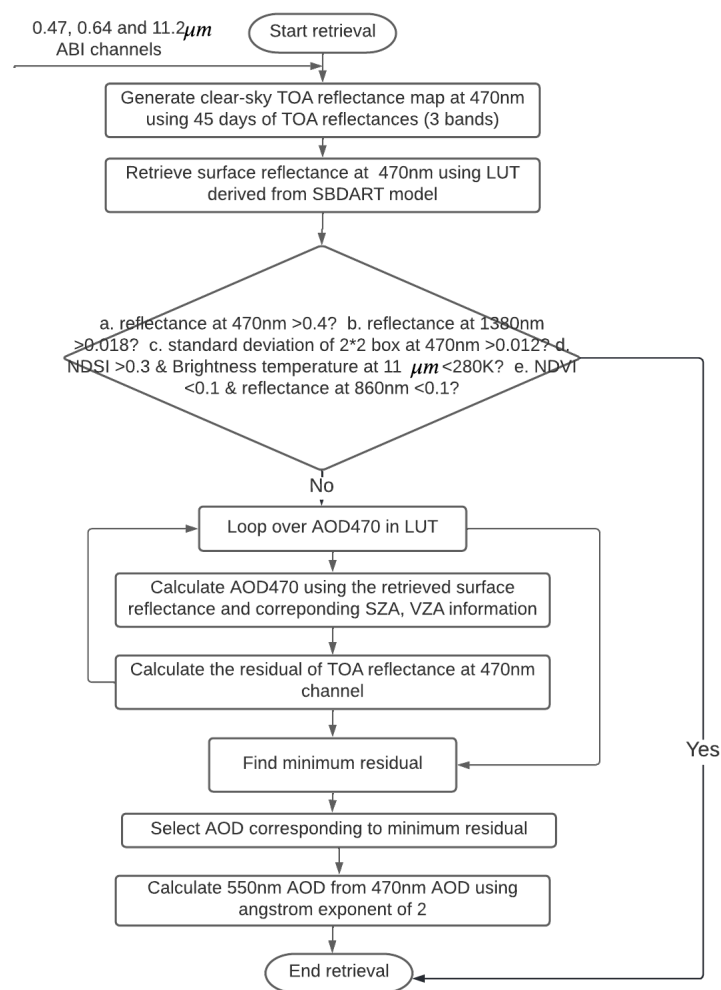


Fig. 1. flowchart of the AOD retrieval illustrating the main processing sections

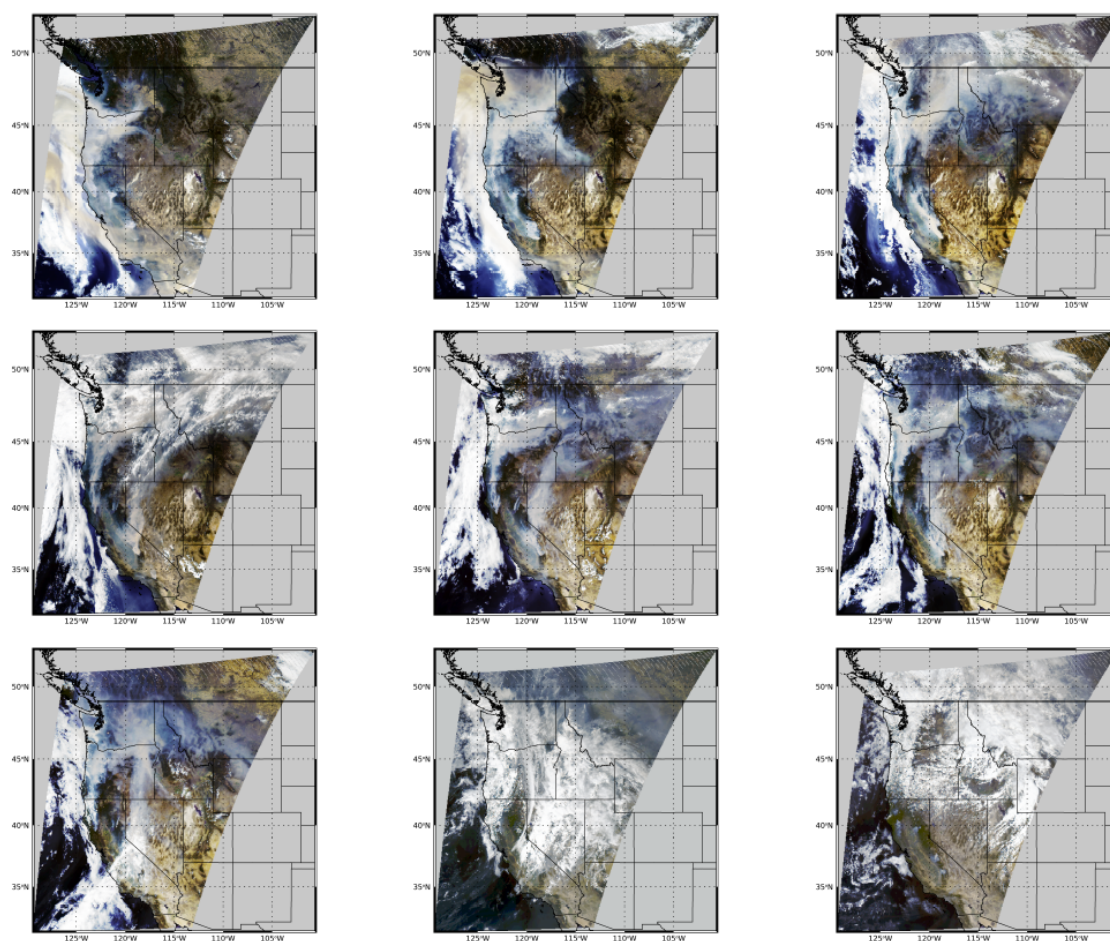


Fig. 2. True color image of wildfire smoke of western US from September 11th to 19th, 2020. Since GOES-R does not have the green band, we use $0.45 \times \text{red} + 0.1 \times \text{veggie} + 0.45 \times \text{blue}$ to calculate a "fake" green channel to show the RGB image (red- $0.67\mu\text{m}$ channel, veggie- $0.86\mu\text{m}$ channel, blue- $0.47\mu\text{m}$ channel).

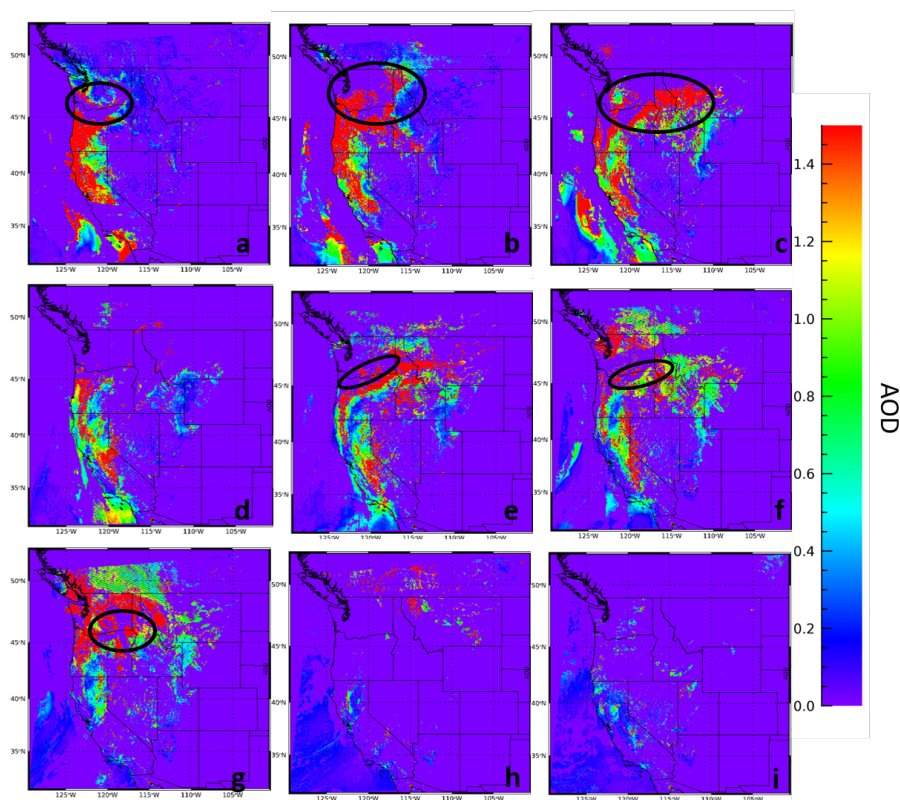


Fig. 3. GOES-R ABI level2 AOD data of the wildfire event in western US from September 11th to 19th, 2020. Comparing with previous true color image of the same time, the thick smoke area (center of the smoke) is missing a large amount of AOD values. The red color indicates AOD of 1.5 and higher.

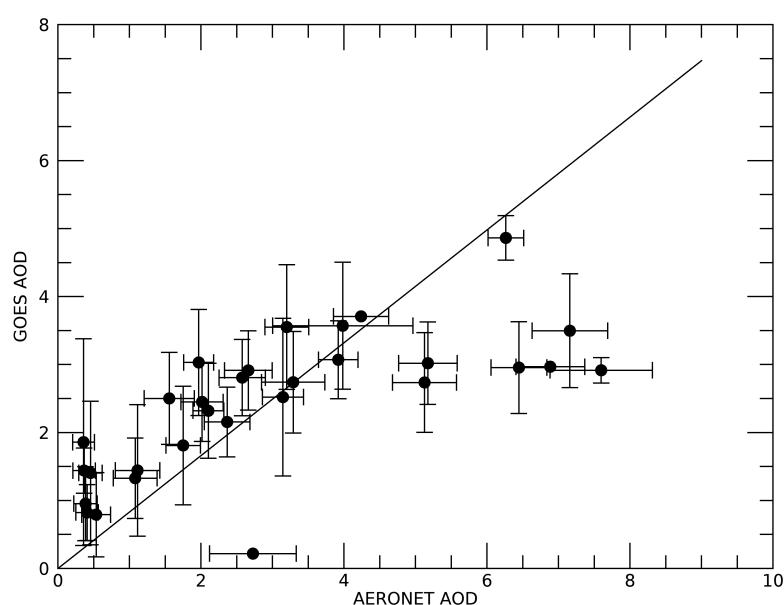


Fig. 4. 3-hour mean AEROET AOD vs. GOES AOD for the 9-day period. The GOES AOD is calculated by averaging all valid AOD values within a 0.3-degree distance (a circle with radius of 0.3 degree). GOES AOD are normally larger than AERONET observations, and the linear relationship of the two: $GOES\ AOD = 1.7 \times AERONET\ AOD + 0.15$. The black reference line indicate the Angstrom exponent of 2. Only when both AERONET and GOES make observations are shown on this figure.

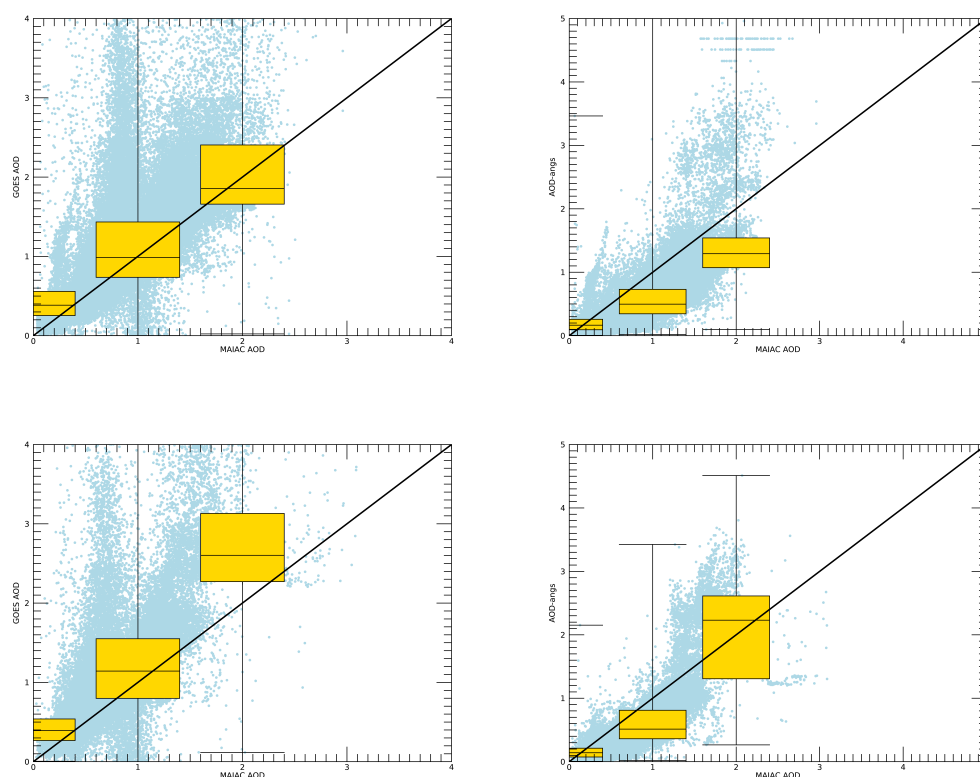


Fig. 5. AOD comparison between MAIAC and GOES (left column), MAIAC and AOD-angs (right column) on September 13th (first row) and 17th (second row) in 2020. Only data points have both valid MAIAC AOD and GOES OAOD values less than 4 are shown here. Due to surface albedo retrieval and different aerosol properties we use, AOD-angs has lower AOD retrieval values than GOES OAOD for same pixels, which is the reason for lower AOD values in the right panel. From the box and whisker plots, GOES OAOD tends to have larger variance.

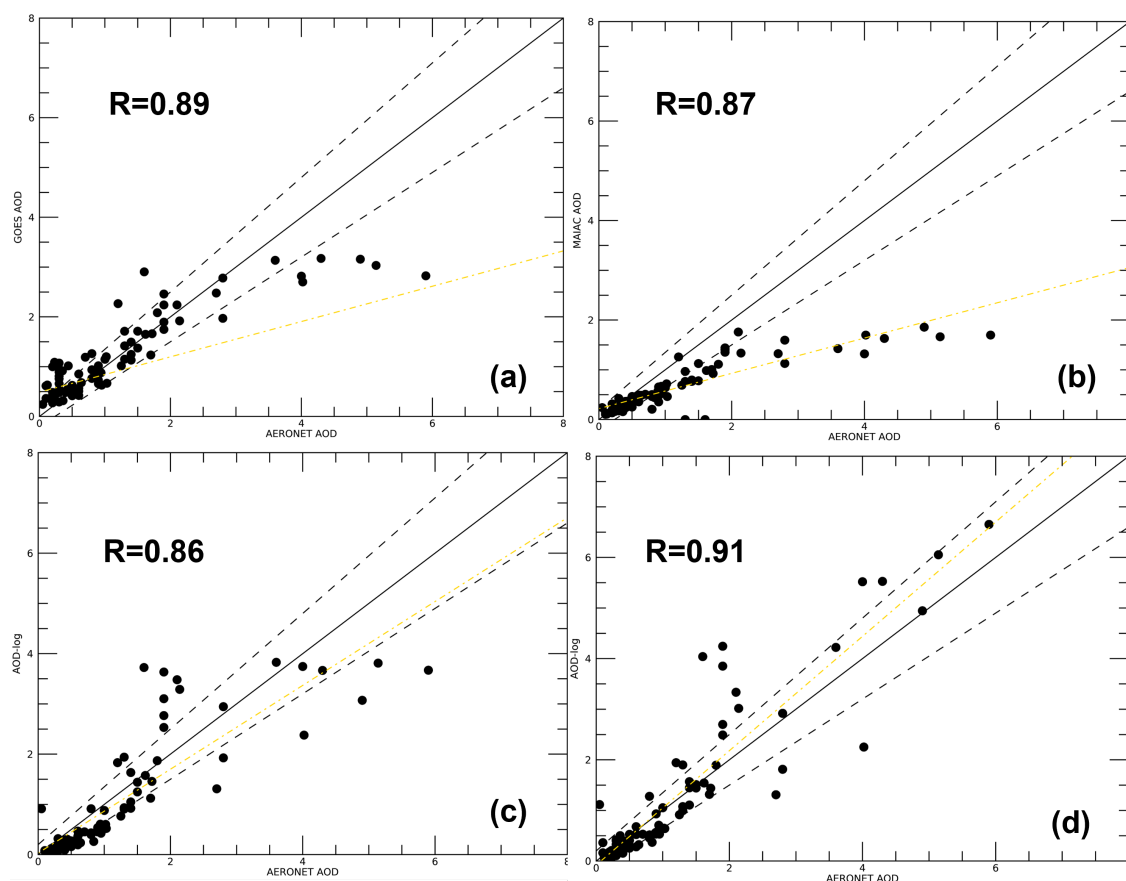


Fig. 6. Validation of satellite AOD with AERONET AOD (a)GOES (b)MAIAC (c)AOD-angs (d)AOD-log. We use AERONET 500nm and 675nm to calculate the Angstrom exponents (AE) of individual sites and convert 500nm AOD to 550nm AOD using the AE. The yellow dotted line is the regression line.

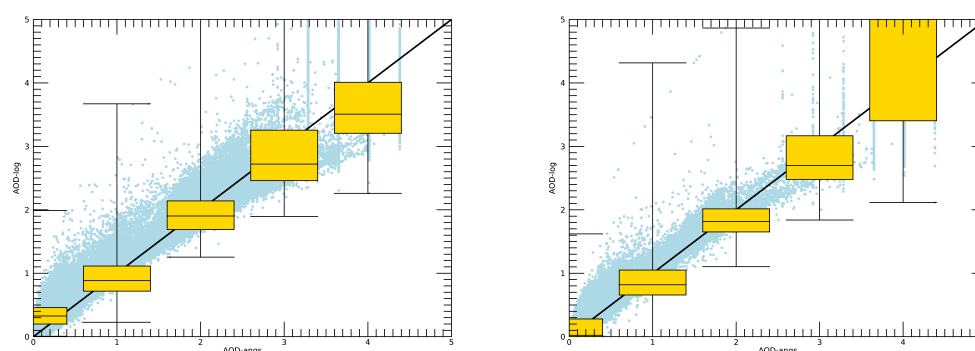


Fig. 7. AOD comparison between AOD-angs and AOD-log on September 13th (left) and 17th (right) in 2020.

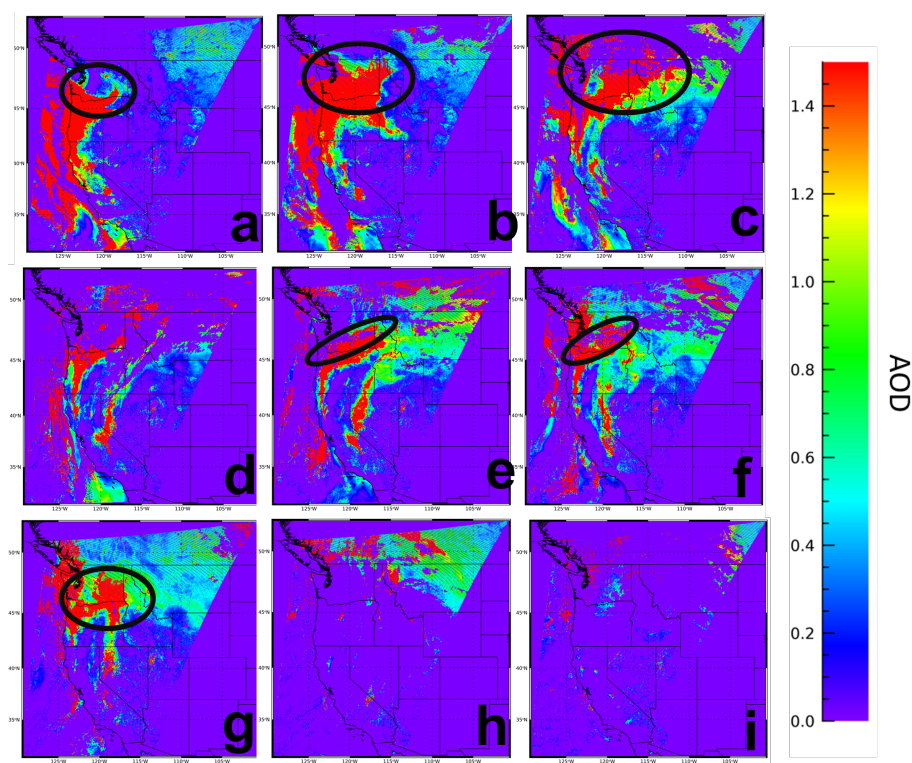


Fig. 8. AOD-log from September 11th, 2020 (20UTC) to September 19th, 2020 (20UTC). The cloudy pixels are masked out using internal tests in GOES algorithm. The 550nm AOD is calculated from the 470nm and 640nm AOD.

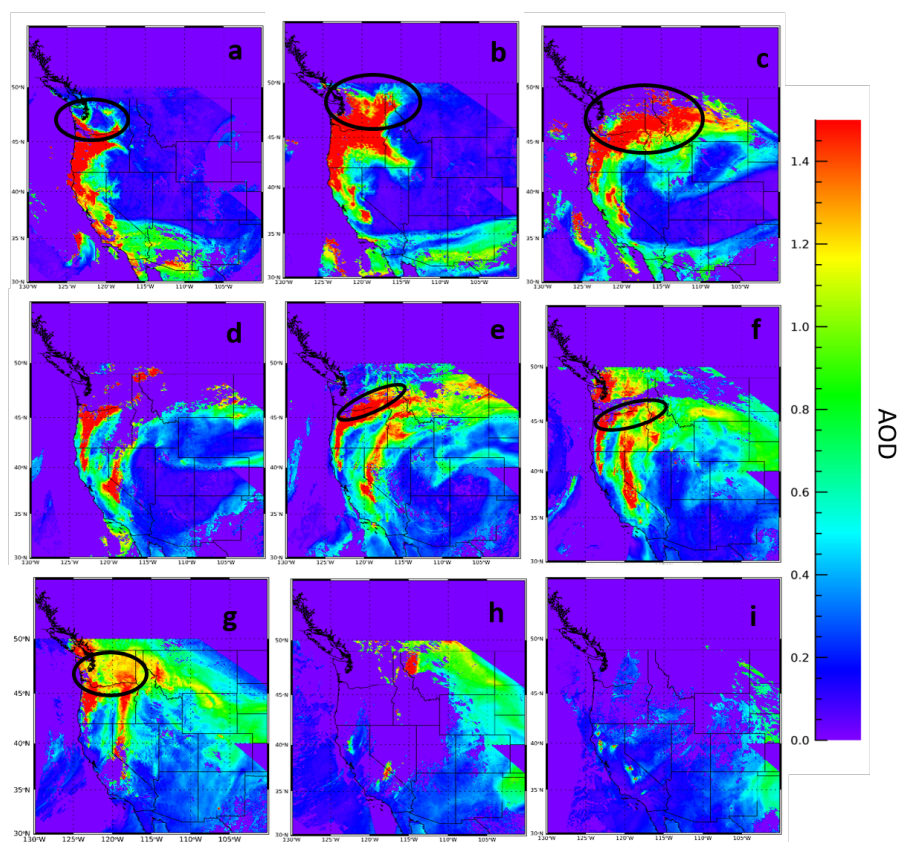


Fig. 9. MAIAC AOD at 550nm from September 11th to 19th in 2020.



Date	Model	R	RMSE	median bias	accuracy within ± 0.5
Sep-11	OAOD vs. MAIAC	0.81	0.43	-0.2	86%
	AOD-angs vs. MAIAC	0.81	0.55	0.07	82%
Sep-12	OAOD vs. MAIAC	0.85	0.52	-0.12	80%
	AOD-angs vs. MAIAC	0.82	0.57	0.09	79%
Sep-13	OAOD vs. MAIAC	0.8	0.41	-0.3	84%
	AOD-angs vs. MAIAC	0.69	0.56	0.1	81%
Sep-14	OAOD vs. MAIAC	0.83	0.38	-0.29	83%
	AOD-angs vs. MAIAC	0.75	0.49	0.08	86%
Sep-15	OAOD vs. MAIAC	0.85	0.35	-0.28	90%
	AOD-angs vs. MAIAC	0.78	0.51	0.1	84%
Sep-16	OAOD vs. MAIAC	0.87	0.37	-0.32	87%
	AOD-angs vs. MAIAC	0.75	0.51	0.16	85%
Sep-17	OAOD vs. MAIAC	0.84	0.35	-0.27	92%
	AOD-angs vs. MAIAC	0.77	0.55	0.18	82%
Sep-18	OAOD vs. MAIAC	0.88	0.25	-0.14	95%
	AOD-angs vs. MAIAC	0.80	0.44	-0.08	90%
Sep-19	OAOD vs. MAIAC	0.59	0.22	-0.13	97%
	AOD-angs vs. MAIAC	0.47	0.47	-0.08	90%

Table 3. Correlation coefficients, root mean squared error (RMSE), median bias and accuracy within ± 0.5 between AOD-angs, GOES and MAIAC AOD from September 11th to 19th

Model	R	RMSE	Median bias	Accuracy within EE ($\pm(0.2+0.15AOD)$)
AOD-angs	0.86	0.65	-0.21	57%
AOD-log	0.91	0.64	-0.04	70%
MAIAC AOD	0.87	0.98	-0.27	60%
OAOD	0.89	0.61	0.1	66%

Table 4. Statistics of different AOD products validation with AERONET AOD